

XU, W., WANG, S., FERNANDEZ, C., YU, C., FAN, Y. and STROE, D.-I. 2020. High-precision state of charge estimation for the power lithium ion batteries by introducing an improved extended Kalman filtering algorithm with complex varying temperatures. In *Proceedings of 5th Advanced robotics and mechatronics international conference 2020 (ICARM 2020), 18-21 December 2020, Shenzhen, China [virtual conference]*. Piscataway: IEEE [online], pages 700-705. Available from: <https://doi.org/10.1109/ICARM49381.2020.9195316>

# High-precision state of charge estimation for the power lithium ion batteries by introducing an improved extended Kalman filtering algorithm with complex varying temperatures.

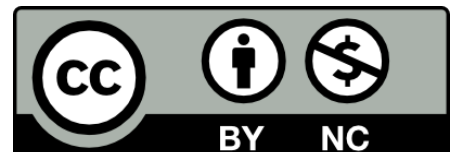
XU, W., WANG, S., FERNANDEZ, C., YU, C., FAN, Y. and STROE, D.-I.

2020

© 2020 IEEE. Personal use of this material is permitted. Permission from IEEE must be obtained for all other uses, in any current or future media, including reprinting/republishing this material for advertising or promotional purposes, creating new collective works, for resale or redistribution to servers or lists, or reuse of any copyrighted component of this work in other works.

OpenAIR  
@RGU

This document was downloaded from  
<https://openair.rgu.ac.uk>



# High-Precision State of Charge Estimation for the Power Lithium Ion Batteries by Introducing an Improved Extended Kalman Filtering Algorithm with Complex Varying Temperatures

Wenhua Xu, Shunli Wang, Carlos Fernandez, Chunmei Yu, Yongcun Fan, Daniel-Ioan Stroe

**Abstract**— Accurate estimation of the state of charge is important for the rational use of lithium ion batteries and the development of electric vehicles. In order to solve the problem that the internal parameters of lithium battery are greatly affected by the temperature change, which makes the estimation of state of charge inaccurate, a new method based on different temperature is proposed. The improved extended Kalman filter algorithm is applied to estimate and track the state of charge at different temperatures and working conditions. The experimental results show that the established estimation model can better estimate the state of charge of lithium battery with fast convergence rate, and can estimate the battery state of different working conditions at different temperatures. The tracking effect is good and the estimation error is controlled within 0.03%.

## I. INTRODUCTION

Power lithium battery has the advantages of simple structure, energy saving and cleanness, and has been widely applied and developed in the field of new energy. Accelerating the development of the electric vehicle industry has become the world consensus [1]. As the main battery of electric vehicles, the health status detection of lithium battery has been paid more and more attention [2]. Among them, the estimation of the State of Charge (SOC) of lithium battery is very important [3]. Accurately estimating the SOC of the battery can provide the driver with reference to predict the remaining mileage.

The internal chemical reaction of lithium battery is complex and variable, and the operating characteristics are highly nonlinear. Therefore, the SOC of the battery is estimated indirectly mainly through the external characteristics. Experts in related fields have conducted in-depth research on SOC estimation of lithium battery. SOC dynamic tracking can be realized by Ampere-hour (Ah) integration, and the operation is simple, but this method is difficult to measure the initial state of SOC. Open circuit voltage method can provide initial value for lithium battery, but it takes a longer time to place. It only applies to the initial

and final stages of battery charging. Therefore, some researchers have proposed combining the open circuit voltage method with the Ah integration method to complete the SOC initial value estimation and to realize the dynamic prediction of the SOC. However, with the increase of time, the above method still inevitably has an SOC cumulative estimation error. Later, some scholars proposed other intelligent algorithms, such as Kalman Filter (KF) algorithm, neural network algorithm and some improved algorithm [4], [5], [6]. Chen et al. [7] estimated SOC of lithium battery through particle filter. Li et al. [8] used combination methods to estimate SOC.

The equivalent modeling of lithium battery is the basis of its state estimation, which has important significance in the battery management system [9]. Common battery models in current applications include electrochemical model, neural network model, and equivalent circuit model [10]. Electrochemical model can be used to investigate the internal chemical mechanism and chemical reaction of lithium battery [11]. The estimation accuracy is high but the corresponding calculation amount is large, which is not suitable for engineering applications [12]. Based on a significant amount of experimental data, the neural network model estimates SOC through input and output relationships [13]. Because it has a strong dependence on experimental data, the lack of experimental data will lead to a large estimation error. The equivalent circuit model uses circuit reactions to simulate the reaction inside the battery [14]. The equivalent circuit model is more intuitive and easier to process, and the amount of calculation is moderate, and the parameters of the model are easy to identify, which is suitable for simulation experiments [15]. Common battery equivalent circuit models in current applications include internal resistance equivalent model, RC equivalent model, Thevenin equivalent model, and PNGV equivalent model. There are many improved models in recent years [16], [17], [18]. De Sutter et al. [19] conducted extensive parameterization studies on fractional differential model. Meng et al. [20] proposed a dynamic linear battery model establishment method. Kim et al. [21] studied an enhanced hybrid battery model. Drummond et al. [22] established the Doyle-Fuller-Newman electrochemical model.

The above methods do not consider the effect of temperature on battery state, but the change of temperature has a great influence on battery capacity and internal resistance, which will affect the estimation effect of the SOC [23]. In view of the above situation, based on the SOC estimation at different temperatures, the influence of temperature on the parameters of the battery model is considered, and the influence of high and low temperature on

The work was supported by National Natural Science Foundation of China (No. 61801407), China Scholarship Council (No. 201908515099), Sichuan Province Science and Technology Support Program (No. 2019YFG0427). Thanks to the sponsors. CF would like to express his gratitude to PALS for its support.

W. H. Xu, S. L. Wang, C. M. Yu, and Y. C. Fan are with School of Information Engineering, Southwest University of Science and Technology, Mianyang 621010, China (Corresponding author: S. L. Wang).

C. Fernandez is with School of Pharmacy and Life Sciences, Robert Gordon University, Aberdeen AB10-7GJ, UK.

D. I. Stroe is with Department of Energy Technology, Aalborg University, Pontoppidanstraede 111 9220 Aalborg East, Denmark.

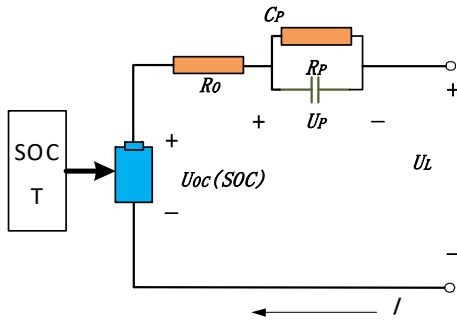


Figure 1 The Thevenin model

battery internal parameters is analyzed. On this basis, a variable gain coefficient is introduced to modify the extended Kalman filter algorithm to reduce the influence of temperature on state estimation. Firstly, the Thevenin model is constructed, and the parameters of the established model are identified by experiment. Finally, the improved algorithm is implemented in MATLAB/Simulink and the estimation effect of the algorithm is analyzed.

## II. MATHEMATICAL ANALYSIS

### A. Equivalent Circuit Modeling

In order to accurately obtain the current SOC of the battery, it is necessary to select a suitable equivalent model. Although the internal resistance equivalent model is simple, it doesn't take into account the transient characteristics of the electrochemical reaction process of the battery, and cannot accurately characterize the change process. The PNGV model has a high accuracy due to the consideration of self-discharge effect. However, the introduction of series capacitance makes the method prone to cumulative errors in long-term simulation. Because the Thevenin model has a simple structure, parameters are easy to identify, and the polarization phenomenon of the battery is considered, the Thevenin model is chosen to describe the dynamic characteristics of the battery. It is shown in Fig. 1.

Among them,  $U_{OC}$  indicates the open circuit voltage.  $R_o$  indicates the ohmic internal resistance of the battery.  $R_p$  and  $C_p$  indicate the polarization internal resistance and capacitance of the battery. According to the equivalent model, the state space equation is obtained as shown in Eq. (1).

$$\begin{cases} U_L = U_{oc} - IR_o - U_p \\ I(t) = C_p \frac{dU_p}{dt} + \frac{U_p}{R_p} \end{cases} \quad (1)$$

### B. Improved Extended Kalman Filter Algorithm

The Extended Kalman Filter (EKF) algorithm is actually a linearization process of a nonlinear system. The value of the next moment is estimated by the previous time, and the state variables are continuously updated by the observation values of the system input and output, thereby achieving the optimal estimation. In the estimation process, the Taylor expansion is used to expand the system equations of the lithium battery, then the first-order linearization model is obtained after the

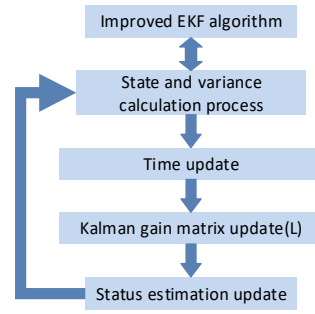


Figure 2 IEKF algorithm flow chart

high-order term is removed. After obtaining the linearized model, the Kalman filter algorithm with variable gain coefficient is used to estimate the SOC. The Improved Extended Kalman Filter (IEKF) algorithm is shown in Fig. 2.

The extended Kalman algorithm is an improvement of the classical Kalman algorithm. The filtering algorithm is used to estimate the current state and is suitable for discrete nonlinear systems. The improved EKF algorithm includes temperature coefficient and variable gain parameters to consider the effect of temperature change on battery capacity, and the variable gain coefficient is used to IEKF.

Since temperature has an impact on capacity, the temperature coefficient is introduced to correct the error, and the traditional Ah integration method is improved to make the calculation of SOC more accurate, as shown in Eq. (2).

$$SOC(t) = SOC(t_0) - \int_0^t \frac{\eta i(t)}{K_t Q_N} dt \quad (2)$$

In the formula,  $K_t$  is the temperature coefficient, which is the ratio of capacity at current temperature to that at standard temperature.  $Q_N$  is the rated capacity. According to the Thevenin model, the state space expression is as shown in Eq. (1), and the discretization is as shown in Eq. (3).

$$\begin{cases} x(k|k-1) = A_{k-1}x(k-1) + B_{k-1}i_{k-1} + w_k \\ y(k|k-1) = C_k x(k|k-1) - R_o i_k + v_k \end{cases} \quad (3)$$

$$\begin{cases} A_k = \begin{pmatrix} 1 & 0 \\ 0 & e^{-t/\tau} \end{pmatrix} \\ B_k = \begin{pmatrix} -\frac{t}{K_t Q_N} \\ R_2(1 - e^{-t/\tau}) \end{pmatrix} \\ C_k = \left( \frac{\partial u_{oc}}{\partial soc} \quad -1 \right) \Big|_{x_k = \hat{x}_k} \end{cases} \quad (4)$$

where,  $w_k$  and  $v_k$  are mutually independent Gaussian white noise. For Eq. (3), in order to use Kalman filtering, the first-order Taylor expansion of the equation is carried out, and the values of  $A_k$ ,  $B_k$ , and  $C_k$  are obtained as shown in Eq. (4). The Kalman filter with variable gain is applied to the linearized model, and the iterative process of the improved extended Kalman filter is as shown in Eq. (5).

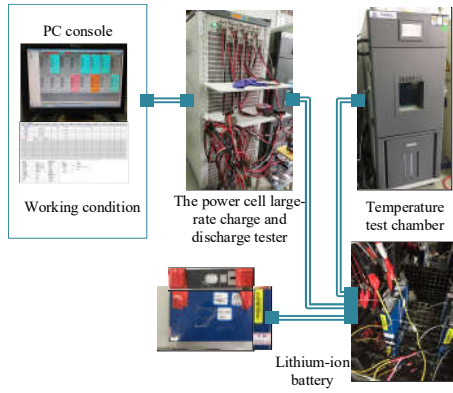


Figure 3 The experiments equipment

$$\begin{cases} x(k|k-1) = A_{k-1}x(k-1) + B_{k-1}i_{k-1} \\ P(k|k-1) = A_{k-1}P(k-1)A_{k-1}^T + Q_k \\ \hat{K}_k = P(k|k-1)C_k^T [C_k P(k|k-1)C_k^T + R_k]^{-1} \\ K_k = L \cdot \hat{K}_k \\ x_k = x(k|k-1) + K_k [U_L(k) - C_k x(k|k-1) - R_o i(k)] \\ P_k = (I - K_k C_k) P(k|k-1) \end{cases} \quad (5)$$

where  $P$  is the mean square error and  $K$  is the Kalman gain.  $L$  is the variable gain coefficient.  $I$  is an identity matrix.  $Q$  and  $R$  are the variances of  $w$  and  $v$ .

### III. EXPERIMENTAL ANALYSIS

The parameters of the Thevenin equivalent model are identified and the characterization effect of the model on the battery is verified by experiments. Under a variety of initial SOC conditions, the influence of different initial conditions on the estimation result is studied, and the convergence of the initial estimation algorithm is observed. Experimental analysis is carried out under a variety of simulation conditions. The influence of the change of working conditions on the estimation effect of the model, the convergence in the estimation process and the tracking of the real data are studied. The reliable verification of the effect of the estimation model is achieved.

#### A. Test Equipment and Procedures

The Ternary lithium ion battery is selected for testing. The battery rated capacity is 50 Ah, and the actual capacity is calibrated at different temperatures. The instruments used in the test include the power cell large-rate charge and discharge tester, a three-layer temperature test chamber (BTT-331C) and other supporting experiments equipment, as shown in Fig. 3.

The battery is aging due to some reasons such as recycling, so that the actual capacity and the calibration capacity of the battery will be greatly deviated. The real discharge capacity is of great significance to the SOC estimation of the lithium ion battery, so the capacity calibration of the lithium ion battery should be carried out first.

The battery is subjected to Hybrid Pulse Power Characterization (HPPC) at different temperatures, and the battery model parameters are obtained by analyzing the operating characteristics of the battery during operation.

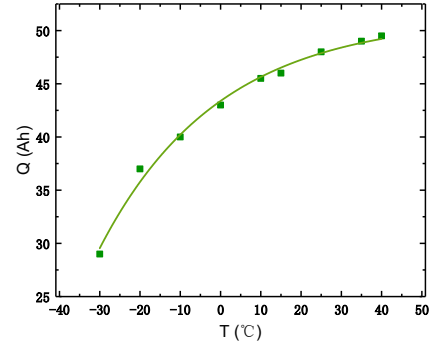


Figure 4 Lithium battery capacity with temperature curve

#### B. Experimental Result

The experiments are conducted at different temperatures. First, the capacity of lithium ion battery is calibrated to obtain the actual capacity at different temperatures. The curve of capacity changing with temperature is shown in Fig. 4.

According to the curve of capacity changing with temperature, the low temperature will reduce the available capacity, while the high temperature will increase the activity of the battery material, resulting in a large available capacity. However, the excessive high temperature will damage the battery. The experiment shows that the change of temperature will make the lithium ion battery capacity change obviously. In order to accurately estimate the state of lithium ion battery, the influence of temperature on its capacity must be considered.

The lithium ion battery is tested with HPPC at different temperatures. The voltage curve of one of the HPPC tests is shown in Fig. 5. It can be seen from the voltage curve in Fig. 5 that the battery voltage at the end of the discharge will gradually stabilize after a long period of time, which means that the internal chemical reaction and thermal effect have basically reached equilibrium. The battery voltage is its open circuit voltage, so the relationship between the open circuit voltage and SOC at different temperatures is obtained as shown in Fig. 6.

In Fig. 6, the open circuit voltage  $U_{oc}$  decreases with the decrease of SOC at different temperatures, and decreases rapidly when the SOC is large. At the same time, it can be seen that temperature has little effect on the open-circuit voltage of lithium battery.

#### C. Parameter identification

Analysis of Figure 6 shows that at the start and the end of discharge at  $t1$  to  $t2$  and  $t3$  to  $t4$ , the voltage at the battery terminal drops sharply under the influence of the ohmic resistance of the battery. During  $t4$  to  $t5$ , the battery voltage rises slowly. At this time, it is zero input effect of RC circuit in the circuit model. In other words, the RC circuit returns energy to the battery circuit after storing energy for a time, leading to the rise of voltage. The ohmic internal resistance and the terminal voltage of the battery can be obtained as shown in Eq. (6).

$$\begin{cases} R = \frac{|U_2 - U_1| + |U_4 - U_3|}{2I} \\ U_0 = U_{oc} - IR_1 e^{-\frac{t}{\tau}} \end{cases} \quad (6)$$

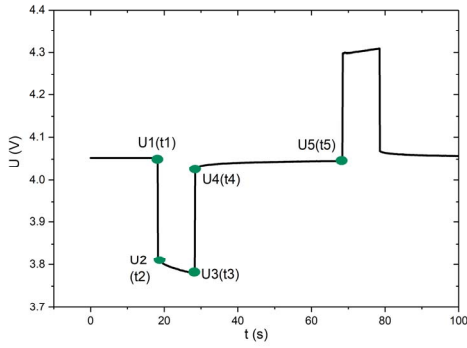


Figure 5 One HPPC experimental voltage curve

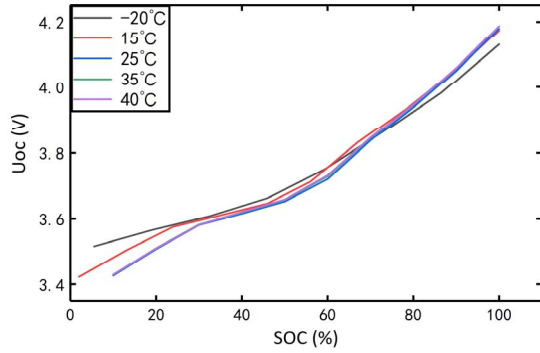


Figure 6 OCV-SOC changes at different temperatures

In the formula,  $I$  is the corresponding current value. The time constant  $\tau_I = R_p C_p$ .

According to Eq. (6), the change of ohmic internal resistance at various SOC stages at varying temperatures can be obtained, as shown in Fig. 7.

In Fig. 7, the ohmic internal resistance decreases with the increase of temperature, and increases when the discharge reaches a certain depth at the same temperature. At the high temperature of 40 degrees, the ohmic resistance is very small. At a low temperature of -20 degrees, the ohmic resistance is large and increases rapidly at a low temperature. The analysis shows that there is no significant change in the ohmic internal resistance at the same temperature, so the average value can be taken.

The  $R_p$  and  $C_p$  values in different SOC shapes at varying temperatures are obtained as shown in Fig. 8. As can be seen from Figure 8 that the polarization resistance decreases with the increase of temperature, which is similar to the ohmic internal resistance. When the discharge depth increases, the polarization resistance will increase. Fig. 8 shows that the polarization capacitance of lithium ion battery increases with the temperature rise.

In order to validate the characterization of the battery voltage in the actual operating conditions of the constructed equivalent circuit model. The real voltage and current data under 25°C the cyclic discharge held condition are imported into the battery equivalent model constructed by MATLAB/Simulink, and the model is verified by combining the previous parameter identification results. The estimated value is compared with the actual terminal voltage value as shown in Fig. 9.

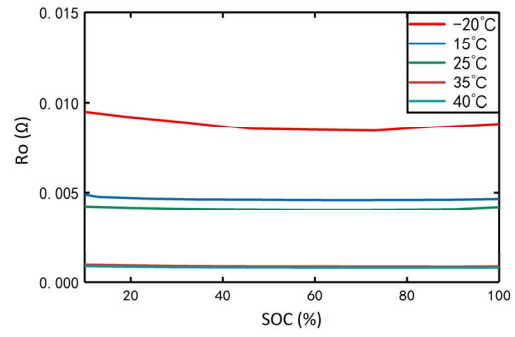


Figure 7 Variation of ohmic resistance with temperature and SOC

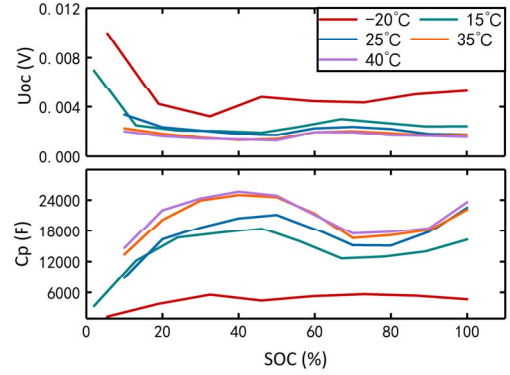


Figure 8 Variation of polarization resistance and capacitance with temperature and SOC

Fig. 9 shows the comparison between the estimated value and the real value when the battery is discharged under the experimental condition of cyclic discharge. Where the red line is the estimated value of the constructed model, while the solid blue line is the real battery terminal voltage. In the Fig. 9, the estimated value has a good tracking effect on the real value, and the estimated error is within 0.07V, which can basically represent the terminal voltage value of the battery at work. It can also be seen from the analysis of the comparison error of the two voltages that the error of the voltage estimation increases at the end of the battery discharge. This is because the battery voltage changes dramatically at the end of the discharge, and the simulation expectation lag behind, which leads to the increase of the estimation error.

#### D. Cycle Charging and Discharging Condition Analysis

Considering that the battery is usually in intermittent discharge state in actual use, and in order to validate the estimation effect at different temperatures, the estimated results are further analyzed under the experimental condition of 35°C cyclic discharge. The estimated result is shown in Fig. 10.

Fig. 10 shows the theoretical calculation value of battery SOC and the estimation value of improved EKF. It can be seen from the figure that this algorithm has a good estimation effect. The estimated deviation is stable within 0.03%, and the overall performance is excellent. What is noteworthy is that when the battery in a suspended state, the SOC estimation error becomes larger. This is because when the battery is in a suspended state, there is a lag in the battery equivalent circuit model, which leads to the larger deviation of SOC estimation.

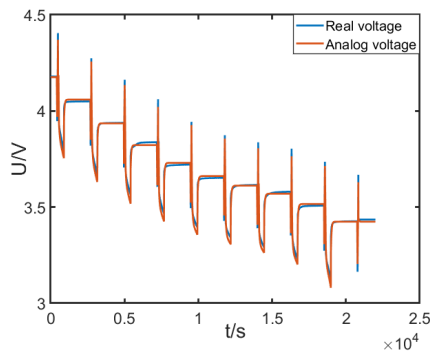


Figure 9 Thevenin equivalent circuit model simulation

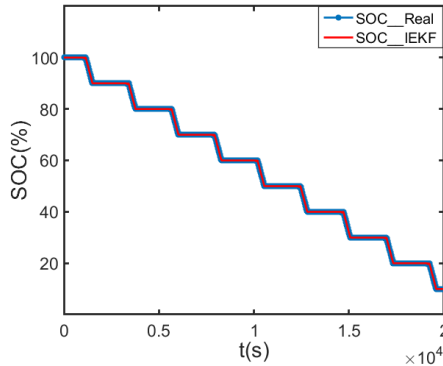


Figure 10 IEKF-SOC estimation under cyclic discharge

### E. DST Condition Analysis

In order to further verify the response of the model to the SOC of the lithium battery under more complex application conditions, the model is validated with custom DST experimental data at 27°C. The experimental voltage and current data of the DST working condition is shown in Fig. 11.

The experiment data are imported into the MATLAB working platform, and the estimation model is analyzed. The results of comparing the SOC value with the theoretical value and the estimation error are shown in Fig. 12.

The battery starts discharging at full charge, and its initial SOC is considered to be 1. As shown in Fig. 12, the overall SOC estimation shows a fluctuation downward trend, which is due to the alternating charge-discharge process during the experiment. Under the condition of DST, IEKF has a good tracking effect on SOC, and the estimated error is within 0.01%, which can better track the battery SOC under this condition.

## IV. CONCLUSION

Accurate SOC estimation of lithium ion battery is the focus and difficulty of lithium battery condition monitoring. In this paper, considering the influence of temperature on the battery state, based on the improved Thevenin model to characterize the state and output characteristics of lithium battery, pulse discharge experiments were conducted at different temperatures to identify parameters, and the relationship between circuit model parameters and lithium battery state and temperature changes was determined. Then the improved extended Kalman algorithm was used to estimate the SOC based on the established model. Simulink

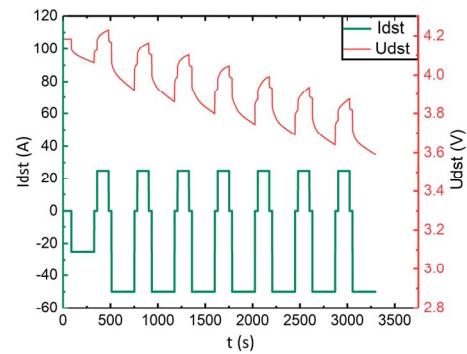


Figure 11 Battery voltage and current curve of DST working condition

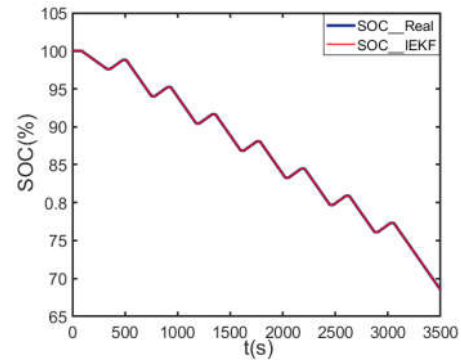


Figure 12 SOC estimation of IEKF under DST condition

model was built on MATLAB, and the experimental data of different temperature conditions were combined for simulation analysis. The results show that the established estimation model can well estimate the SOC of lithium batteries, and can estimate the SOC under varying temperatures and working conditions. The estimation error is controlled within 0.03%, which verifies that the algorithm has high accuracy in the SOC estimation of lithium batteries.

## REFERENCES

- [1] K. M. Winslow, S. J. Laux, and T. G. Townsend, "A review on the growing concern and potential management strategies of waste lithium-ion batteries," *Resources Conservation and Recycling*, vol. 129, pp. 263-277, Feb 2018.
- [2] Y. Wang, J. Tian, Z. Chen, and X. Liu, "Model based insulation fault diagnosis for lithium-ion battery pack in electric vehicles," *Measurement*, vol. 131, pp. 443-451, Jan 2019.
- [3] Y. Wang, C. Liu, R. Pan, and Z. Chen, "Modeling and state-of-charge prediction of lithium-ion battery and ultracapacitor hybrids with a co-estimator," *Energy*, vol. 121, pp. 739-750, Feb 15 2017.
- [4] Y. Wang, C. Zhang, and Z. Chen, "State-of-charge estimation of lithium-ion batteries based on multiple filters method," *Clean, Efficient and Affordable Energy for a Sustainable Future*, vol. 75, pp. 2635-2640, 2015.
- [5] J. Li and M. Liu, "State-of-charge estimation of lithium-ion batteries using composite multi-dimensional features and a neural network," *Iet Power Electronics*, vol. 12, no. 6, pp. 1470-1478, May 29 2019.
- [6] W. Zhao, X. Kong, and C. Wang, "Combined estimation of the state of charge of a lithium battery based on a back-propagation- adaptive kalman filter algorithm," *Proceedings Of the Institution Of Mechanical Engineers Part D-Journal Of Automobile Engineering*, vol. 232, no. 3, pp. 357-366, Feb 2018.
- [7] Z. Chen, H. Sun, G. Dong, J. Wei, and J. Wu, "Particle filter-based state-of-charge estimation and remaining-dischargeable-time prediction method for lithium-ion batteries," *Journal Of Power Sources*, vol. 414, pp. 158-166, Feb 28 2019.
- [8] G. Li, K. Peng, and B. Li, "State-of-charge estimation for lithium-ion

- battery using a combined method,” *Journal Of Power Electronics*, vol. 18, no. 1, pp. 129-136, Jan 2018.
- [9] Y. Zheng, W. Gao, M. Ouyang, L. Lu, L. Zhou, and X. Han, “State-of-charge inconsistency estimation of lithium-ion battery pack using mean-difference model and extended kalman filter,” *Journal Of Power Sources*, vol. 383, pp. 50-58, Apr 15 2018.
- [10] J. Su, M. Lin, S. Wang, J. Li, J. Coffie-Ken, and F. Xie, “An equivalent circuit model analysis for the lithium-ion battery pack in pure electric vehicles,” *Measurement & Control*, vol. 52, no. 3-4, pp. 193-201, Mar-Apr 2019.
- [11] V. Laue, F. Roder, and U. Krewer, “Joint structural and electrochemical modeling: Impact of porosity on lithium-ion battery performance,” *Electrochimica Acta*, vol. 314, pp. 20-31, Aug 10 2019.
- [12] C. Yuan, B. Wang, H. Zhang, C. Long, and H. Li, “State-of-charge estimation of lithium-ion battery based on a novel reduced order electrochemical model,” *International Journal of Electrochemical Science*, vol. 13, no. 1, pp. 1131-1146, Jan 2018.
- [13] C. Chen, R. Xiong, R. Yang, W. Shen, and F. Sun, “State-of-charge estimation of lithium-ion battery using an improved neural network model and extended kalman filter,” *Journal of Cleaner Production*, vol. 234, pp. 1153-1164, Oct 10 2019.
- [14] J. Hidalgo-Reyes, J. Gomez-Aguilar, R. Escobar-Jimenez, V. Alvarado-Martinez, and M. Lopez-Lopez, “Classical and fractional-order modeling of equivalent electrical circuits for supercapacitors and batteries, energy management strategies for hybrid systems and methods for the state of charge estimation: A state of the art review,” *Microelectronics Journal*, vol. 85, pp. 109-128, Mar 2019.
- [15] K. Sato, A. Kono, H. Urushibata, Y. Fujita, and M. Koyama, “Physics-based model of lithium-ion batteries running on a circuit simulator,” *Electrical Engineering In Japan*, vol. 208, no. 3-4, pp. 48-63, Sep 2019.
- [16] L. D. Couto, J. Schorsch, N. Job, A. Leonard, and M. Kinnaert, “State of health estimation for lithium ion batteries based on an equivalent-hydraulic model: An iron phosphate application,” *Journal of Energy Storage*, vol. 21, pp. 259-271, Feb 2019.
- [17] G. S. Misyris, D. I. Doukas, T. A. Papadopoulos, D. P. Labridis, and V. G. Agelidis, “State-of-charge estimation for li-ion batteries: A more accurate hybrid approach,” *Ieee Transactions on Energy Conversion*, vol. 34, no. 1, pp. 109-119, Mar 2019.
- [18] S. Li, H. He, and J. Li, “Big data driven lithium-ion battery modeling method based on sdae-elm algorithm and data pre-processing technology,” *Applied Energy*, vol. 242, pp. 1259-1273, May 15 2019.
- [19] L. De Sutter, Y. Firouz, J. De Hoog, N. Omar, and J. Van Mierlo, “Battery aging assessment and parametric study of lithium-ion batteries by means of a fractional differential model,” *Electrochimica Acta*, vol. 305, pp. 24-36, May 10 2019.
- [20] J. Meng, D. Stroe, M. Ricco, G. Luo, and R. Teodorescu, “A simplified mode based state-of-charge estimation approach for lithium-ion battery with dynamic linear model,” *Ieee Transactions on Industrial Electronics*, vol. 66, no. 10, pp. 7717-7727, Oct 2019.
- [21] T. Kim, W. Qiao, and L. Y. Qu, “An enhanced hybrid battery model,” *Ieee Transactions on Energy Conversion*, vol. 34, no. 4, pp. 1848-1858, Dec 2019.
- [22] R. Drummond and S. R. Duncan, “Observer design for the doyle-fuller-newman li-ion battery model without electrolyte dynamics,” *Journal Of Energy Storage*, vol. 23, pp. 250-257, Jun 2019.
- [23] X. Wang, X. Wei, and H. Dai, “Estimation of state of health of lithium-ion batteries based on charge transfer resistance considering different temperature and state of charge,” *Journal Of Energy Storage*, vol. 21, pp. 618-631, Feb 2019.